minerals

MDPI

Article

Size-Fractionated Weathering of Olivine, Its CO_2-Sequestration Rate, and Ecotoxicological Risk Assessment of Nickel Release

Jos P. M. Vink [1,*] and Pol Knops [2]

[1] Deltares Foundation, Soil and Subsurface Systems, P.O. Box 177, 2600 MH Delft, The Netherlands
[2] PlanBCO2, Rijksstraatweg 128, 7391 MG Twello, The Netherlands
* Correspondence: jos.vink@deltares.nl

Abstract: Olivine, one of the most abundant silicates on earth, thermodynamically captures CO_2 in relevant amounts during its dissolution. Upscaling the use of this mineral as a replacement for sand or gravel may contribute to reduce concentrations of greenhouse gasses in the atmosphere. However, the reliable quantification of weathering rates and prognoses for effects of various environmental conditions on weathering are lacking. This currently inhibits the monitoring, reporting and verification of CO_2 capture and hampers the exploitation of the carbon dioxide removal economy. A mineral dissolution model was developed, and olivine weathering rates were directly coupled to particle sizes of the ground mineral. A particle size-dependent calculation approach, based on the shrinking core model, showed faster weathering rates as compared to a single-size, monodisperse approach. This provided a better underpinning of the prediction of the overall weathering and, consequently, the sequestration rate of CO_2. Weathering of olivine releases nickel, which is incorporated in the mineral. The dissolution model was coupled to advanced biotic ligand models (BLM) for nickel in order to assess potential chronic ecotoxicological risks upon release in the environment. Predicted no-effect concentrations for nickel showed that both the release of Mg and the increase of pH following olivine weathering significantly lowers nickel ecotoxicity.

Keywords: climate change; CO_2; grain size distribution; mineral enhanced weathering; nickel; risk assessment

check for updates

Citation: Vink, J.P.M.; Knops, P. Size-Fractionated Weathering of Olivine, Its CO_2-Sequestration Rate, and Ecotoxicological Risk Assessment of Nickel Release. *Minerals* **2023**, *13*, 235. https://doi.org/10.3390/min13020235

Academic Editors: Fatima Haque and Shakirudeen A. Salaudeen

Received: 9 January 2023
Revised: 2 February 2023
Accepted: 3 February 2023
Published: 7 February 2023

Copyright: © 2023 by the authors. Licensee MDPI, Basel, Switzerland. This article is an open access article distributed under the terms and conditions of the Creative Commons Attribution (CC BY) license (https://creativecommons.org/licenses/by/4.0/).

1. Introduction

Negative CO_2 emissions are necessary to halt the effects of climate change [1]. This not only requires drastic cuts in current emissions, but also the creation of permanent carbon sinks, often referred to as "negative emissions" [2]. Since awareness of climate change has drawn the interest of both the scientific community and policy makers to produce (cost-)effective mitigation measures, much attention has been given to enhanced weathering of alkaline minerals, such as the magnesium silicate olivine [3–10]. Olivine is one of the most common silicates on earth, and its natural ability to react with atmospheric CO_2 to produce carbonates can be exploited in a variety of applications, such as the construction of footpaths, pavements, soil amendment for planting, etc. [11–13]. However, reliable predictions of the actual rate of weathering under specific environmental conditions, and consequently, the quantification of CO_2 sequestration rates, are lacking. Accurate analyses of the efficiency and effects of olivine applications in terrestrial or aquatic conditions are currently hampered, which consequently inhibits both the verification (MRV; measurement, reporting and verification) [14] and economical exploitation (CDR; carbon dioxide removal) [15] of CO_2 capture. The environmental impact of released nickel, which is incorporated in the mineral, is, at best, empirically determined or estimated. For large-scale applications in the environment, the need for accurate risk assessment, applicable for various olivine sources and environmental conditions, is evident.

The weathering reaction of olivine in the presence of CO_2 is irreversible, and has been generally described by Wood and Kleppa [16] and Donaldson [17]:

$$Mg_2SiO_4 + 4CO_2 + 4H_2O \rightarrow 2Mg^{2+} + 4HCO_3^- + H_4SiO_4 \qquad \Delta H = -84\ kJ{\cdot}mol^{-1}$$

The efficiency of this chemical conversion is dependent on environmental variables, such as pH and temperature. The reaction may be followed by the precipitation of Ca/Mg-carbonates, although CO_2 release through carbonate dissolution and/or sulfide oxidation may occur later in time depending on environmental conditions [6,18].

Mineral weathering can be described by the shrinking core model (SCM), which is widely used to describe situations in which solid particles are being consumed, either by dissolution or chemical reaction. As a result, the particles of the material being consumed decline in size [19]. The SCM model is used, for example, in pharmacokinetics [20] and in dissolution-leaching studies [21,22]. Assumptions of the SCM have been described by Safari et al. [23]. SCM assumes particles to be spherical, and that particle diameters shrink proportionally, i.e., depending on surface-to-volume ratio of the spheres. Although the SCM model can, in principle, be applied for mineral weathering, there are practical limitations. Weathering studies almost always assume particles to be monodisperse, which means that all particles in the batch have a uniform size (commonly expressed as P50 or P80). However, pulverized batches of olivine have no uniform size of the intended fraction, but show a large variety of particle sizes, ranging from some micrometers to millimeters or even centimeters. Hangx and Spiers [24] suggested that disregarding the actual particle size distribution may lead to large variations in calculated weathering rates, and hence, the estimation of the CO_2 uptake rate over time periods.

The purpose of this study was to investigate an alternative for the monodisperse approach in shrinking core modelling and to provide a robust coupling with the release of nickel and its ecological toxicity. In order to quantify mineral weathering, we developed the model OWCS V6.3 (olivine weathering and CO_2 sequestration). The model calculates pH-dependent dissolution of olivine, its CO_2 uptake rate, and the amounts of released magnesium and nickel. The model is coupled to advanced chronic toxicity routines to allow for site-specific risk assessment of nickel. In this paper, we report our modelling concepts and scenarios to quantify: (i) size-specific weathering rates of olivine; (ii) the amount of carbon dioxide that is being consumed in the process, and (iii) the risk assessment of released amounts of nickel (Ni) incorporated in the mineral.

2. Materials and Methods

Many studies have reported on the relationship between mineral dissolution rate (r) and pH [25], temperature [26], mineral saturation [27], and surface area [28,29]. Olsen [30] found a strong pH relationship and clear break near pH = 6:

$$\log r_{pH<6} = -0.48\ pH - 6.9$$

$$\log r_{pH>6} = -0.18\ pH - 8.8$$

The rate constant (k) is temperature-dependent and is described using the first-order Arrhenius function:

$$\ln k_T = \ln k_{T \cdot R} - E_a/R\ (1/T - 1/T_r)$$

in which T is absolute temperature (K), R is the universal gas constant (8.314 $J{\cdot}K^{-1}{\cdot}mol^{-1}$), and E_a is the activation energy ($J{\cdot}mol^{-1}$). It should be noted, however, that there is no full agreement in scientific literature concerning "the dissolution rate r" of olivine, given the fact that mineral size distributions and environmental conditions may vary significantly, thus affecting the dissolution kinetics of the studied mineral. Furthermore, the formation of precipitates around particles during weathering may also influence (temporal) dissolution rates. For this study, we used the dissolution rate derived by Vink et al. [31], who used two olivine types in field experiments in soil under ambient conditions. Model parameters for the following calculations were: $\ln k_T = 7.43 \times 10^{-11}\ mol{\cdot}m^2{\cdot}s^{-1}$; T = 295 K; T_r = 283.7 K.

We adopted the Arrhenius principle to each single size fraction of the ground mineral batch. Figure 1 shows the size fractionation of a medium-sized commercial batch of olivine originating from a dunite mine in Pasek, Spain. Grain size distribution was analyzed by laser diffraction (Malvern particle sizer 2000s). Using this grain size distribution, dissolution rates were calculated for each given time step. The elemental composition of olivine was analyzed in triplicate by X-ray fluorescence (XRF, ThermoFisher Scientific USA ARL 9400). Olivine was used in a dose of 1000 kg·ha^{-1}. The amount of olivine added to soil was coupled to a desired surface area in order to calculate dissolved concentrations of (secondary) weathering products in soil pore water. The total volume of pore water was derived from the amount of precipitation and the porosity of the soil. The rate of dissolution was calculated for each time step over a period of 40 years. In each following time step, the remaining mass from the previous time step was subjected to weathering until a fraction was depleted. The following model conditions were applied: rainfall = 750 mm·y^{-1}; $T_{average}$ = 10.7 °C; initial pH = 6.0, variable; pCO_2 = 410 ppm (data from KNMI 2021 annual average); mixing depth = 0.5 m; soil bulk density = 1.7 kg·L^{-1}; porosity = 0.3. Due to soil respiration, pCO_2 in soil was possibly higher than pCO_2 in air, but we assumed the concentration in air to be rate-limiting for the weathering reaction.

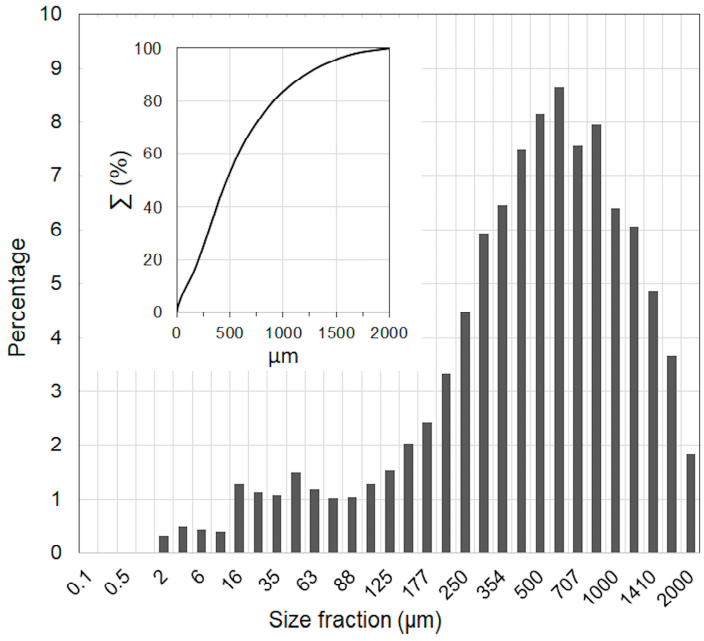


Figure 1. Particle size distribution of a commonly used Spanish olivine batch (0–2 mm). Insert: cumulative size distribution.

Both the particle size distribution of the mineral batch and the applied dose were used to calculate the mass of each size fraction. The progressing reduction of particle diameters was calculated and, consequently, the mass loss in each sequential time step was determined. The chemical composition of the mineral was used for input to calculate released mass of elements such as Mg and Ni per volume unit.

In order to compare the derived weathering rates, the calculations were repeated under the same conditions mentioned before using a monodisperse approach, thus applying a uniform, median value of the grain size. Using the molar conversion from the dissolution reaction, the sequestered CO_2 was calculated. Released Mg and Ni values were calculated and converted from solid to dissolved phase using the Biochem-Orchestra database for chemical partitioning, using pH-dependent nickel sorption to Fe phases and NICA–Donnan sorption to (dissolved) organic matter [32].

The ecotoxicological consequences of the release of nickel due to olivine weathering was approached via higher-tiered risk assessment, using biotic ligand models or

BLMs [33–36]. BLMs are sophisticated toxicity assessment tools, based on metal speciation with competing cations and the binding to biological tissue [37–40]. BLMs compute toxicological "no-effect" concentrations (NOEC) for heavy metals, specifically accounting for chemical speciation and toxicity-based endpoints for biota, e.g., [36]. Competitive interactions between metals and macro-ions (Ca, Na, Mg) for biotic ligand binding and complexation directly relate water composition to metal toxicity. BLMs for Ni are well-studied and have been published in scientific literature for over two decades, e.g., [39]. Their value for regulatory frameworks has been recognized [33,41,42] and laid down in the European Technical Guideline [43] for water quality assessment of metals.

As explained, the nickel BLMs account for chemical speciation (i.e., the distribution of a metal over sorbing and complexing phases) and water composition (i.e., dissolved organic matter, pH, concentrations of macro-ions). Based on these environmental variables, free metal ion activities (FIA) were calculated and predicted no-effect concentrations (PNEC) were derived using the concept of species sensitivity distribution [44] for a range of biota of various trophic levels. For nickel, the toxicity database from the nickel Risk Assessment Report [44] consists of 233 chronic toxicity datapoints for 28 aquatic species. Simplified routines of the BLM models [45] were used in the software tool PNEC-pro V6 [46] and were coupled to the OWCS weathering model. In this way, release and ecotoxicological risk assessment of nickel was directly coupled to time-dependent weathering of olivine (Figure 2).

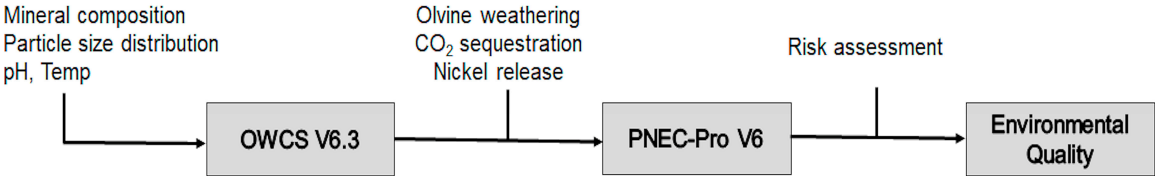


Figure 2. Schematization of model procedures. The weathering rate, based on actual particle size distribution and environmental conditions, is coupled to a BLM toxicity module to provide an environmental risk assessment of released nickel.

3. Results and Discussion

3.1. OWCS Model

The chemical composition of the studied olivine batch is shown in Table 1. The composition is typical for the olivine deposits of this mine. Kremer et al. [47] reported geological characterizations for dunite sources in Europe. Our data show that the olivine from the Spanish mine has a slightly lower magnesium and nickel content, and contains slightly more Al, Ca, V, Sr, and S compared to, for example, Norwegian formations. Applying the shrinking core model to each grain size class, the dissolution of each size class over time was calculated. This is shown quantitatively in Table 2.

Table 2 shows both the initial and the remaining mineral mass per size fraction over time. The smallest size fractions (<8 µm) rapidly decreased in diameter because of their relatively large surface-to-volume ratio and dissolved within the first five years (diameter = 0 µm). This was followed by the second-smallest size fractions in progressing time intervals. The larger particle size fractions exerted a relatively small contribution on the overall weathering—only 13% of the largest particle size class dissolved after 40 years. Overall, 48% of the total dose dissolved after this time period.

Table 1. Geochemical composition of olivine derived from XRF.

Compound	**Mass %**	**St. Dev.**
SiO_2	40.86	±0.01
MgO	35.11	±0.04
Fe_2O_3	7.89	±0.01
Al_2O_3	2.82	±0.01
MnO	0.13	±0.00
Na_2O	0.06	±0.01
TiO_2	0.05	±0.00
CaO	2.15	±0.05
K_2O	0.08	±0.01
P_2O_5	0.01	±0.00
Total	89.16	±0.01
Elements	$mg \cdot kg^{-1}$	
Cr	2281	±62.4
Ni	1301	±0.6
Sr	32.2	±0.64
Zr	158.8	±1.3
Ba	35.8	±13.5

Table 2. Particle diameter (µm) per size class over a weathering period of 40 years and an original mass of 1000 kg. After this period, the smallest size classes have been depleted, and 519 kg olivine remains.

	Years of Weathering										
	0	**1**	**3**	**5**	**10**	**15**	**30**	**40**	**Original Mass (kg)**	**Remaining Mass (kg)**	**Dissolved (%)**
Diameter	**2000**	2000	1993	1989	1982	1971	1946	1928	55	48	13%
	1410	1410	1407	1403	1398	1394	1377	1361	109	90	17%
	1000	999	993	989	982	971	946	928	144	110	24%
	707	706	700	696	689	678	653	635	243	156	36%
	420	419	413	409	402	391	366	348	199	90	55%
	250	249	243	239	232	221	196	178	102	23	77%
	150	149	143	139	132	121	96	78	49	2	97%
	88	87	81	77	70	59	34	16	33	0.0	100%
	50	49	43	39	32	21	0	0	37	0.0	100%
	16	15	9	5	0	0	0	0	13	0.0	100%
	8	7	1	0	0	0	0	0	16	0.0	100%
								∑	1000	519	48%

Figure 3 shows the quantitative effect of using the step-wise dissolution per particle fraction compared to a monodisperse approach. From the data of Figure 1, a P50 median value of 480 µm was derived. The difference between the two approaches is expressed by the statistical error δ over time. The statistical error estimates the variability across multiple time steps ("samples") of two different calculations ("populations") [48]. Early time steps yield large variations, due to the significant influence of very fine particles in the overall dissolution rate. The total error of neglecting this effect added up to 90% in this case, with the major part in the first decennium, which is approximately a factor of two between the two methods.

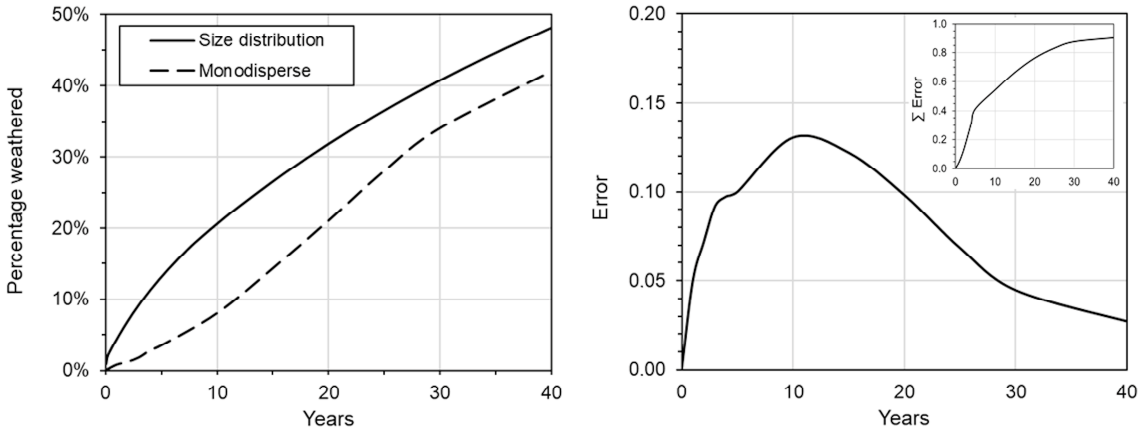


Figure 3. Left: comparison between calculated weathering for monodisperse particles (dotted line) and using the actual particle size distribution (solid line). **Right**: the statistical error δ over time is the coefficient of variation by which the calculated data differ from the expected values, which adds up to 90%.

The capture and cumulative sequestration of carbon dioxide CO_2 following the dissolution reaction and the kinetic size-dependent dissolution of olivine is presented in Figure 4 (left). As shown in Table 2, weathering of all applied olivine was not complete after 40 years, and differences occurred when larger size fractions were left unconsumed in this time period. The complete dissolution of all size fractions was calculated at 250 years, resulting in an overall CO_2 capture of 1.170 kg per ton olivine.

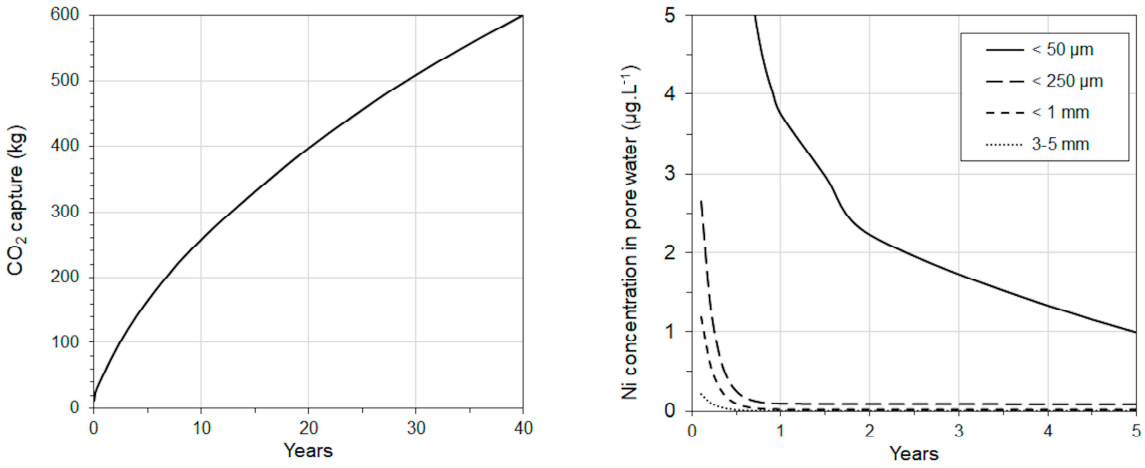


Figure 4. Left: calculated CO_2 capture over time as a result of particle-size-dependent dissolution of olivine. **Right**: the effect of particle size on the release kinetics of nickel in the first 5 years.

The effect of particle size on the release of nickel is shown in Figure 4 (right). The ultra-fine particles (<50 µm) showed the fastest nickel release, as a result of large surface-to-volume ratio, allowing for fast chemical reaction. Hence, nickel was released in a relatively shorter time period compared to the larger fractions. The scenario presented here clearly demonstrates the relation between particle size, its reaction rate, and subsequent nickel release. Renforth et al. [49] performed 1 m soil column percolation tests with olivine amended soils. Olivine of Norwegian origin was used, containing 3 g Ni·kg^{-1} in a dose 10 times larger than applied in our study and using a Hoagland nutrient solution with equivalent pH for percolation. Despite this significantly higher dosage of olivine, and a 2.5 higher nickel content compared to the Spanish mineral used in our study, nickel concentrations in the effluent did not exceed detection limits over the course of the five-month experiments.

3.2. PNEC-Pro Model

The general impact of secondary weathering products of olivine on ecosystems has been reported by many authors [6,7,9,49–55]. Possible risks of the release of nickel in the environment have been addressed by Haque et al. [56], who derived a theoretical geoaccumulation index of Ni and proposed a maximum dose of olivine to soil of 11.3 $kg \cdot m^{-2}$. It should be noted that the olivine used by Haque et al. contained 0.3% Ni; with the olivine used in this study, the maximum amount could roughly be doubled. In addition, it is widely agreed that accumulation of Ni by biota is primarily regulated via the (free) dissolved fraction, not total content [45,57–59]. When nickel is released from olivine due to weathering, a redistribution occurs over a multitude of adsorbing and complexing soil constituents. Over time, sorption and complexation reactions to soil constituents occur, and pore water concentrations decline. According to the speciation calculations performed here, a major part of released nickel is strongly bound to iron and manganese (hydr)oxides (28%), carbonates (23%), and organic matter (20%). The residual 29% is attributed to the exchangeable phase supplying the dissolved concentrations in the pore water phase. For nickel toxicity assessment, we used the model PNEC-pro V6, which is adopted in the EU guidelines for higher-tiered water quality assessment [43]. The BLM-based model predicts the concentrations for which no chronic toxic effects are expected. These concentrations may be compared to generic environmental quality standards for surface waters. The model was used to: (i) calculate no-effect concentrations of nickel and (ii) quantify the effect of released magnesium and intrinsic pH on toxicity endpoints.

3.3. Coupling OWCS and PNEC-Pro

We used the cross-validated BLM model for nickel of Verschoor et al. [45] and applied the transfer functions from the software PNEC-pro V6 [46]. This was coupled to the weathering and dissolution model routine, which provides time-dependent release of nickel (Figure 4, right). Calculated nickel concentrations were used for input for the case described previously. As explained earlier, dissolution of olivine results in a release of magnesium (Mg) and a (temporary) increase of pH due to the production of (bi)carbonates. Nickel BLMs specifically account for these environmental parameters to calculate PNECs. The effect of released magnesium (as a result of progressing olivine weathering) on the chronic toxicity of dissolved nickel is shown in Figure 5. We assumed constant concentrations of Ca = 40 mg/L^{-1} and a dissolved organic carbon (DOC) concentration = 5 $mg \cdot L^{-1}$. With increasing [Mg], the value of $PNEC_{Ni}$ increased significantly, indicating a decrease in chronic toxicity for dissolved nickel. In other words: olivine weathering decreases nickel toxicity. The same trend, but to a slightly lesser extent, was observed for the pH: an increase by 1 pH unit grossly doubled the PNEC value for nickel. The development of the free ion activity model (FIAM) for metals clearly recognized that the presence of protons and cations (e.g., Ca^{2+}, Mg^{2+}, H^{+}) in solution affects the accumulation and toxicity by competing for toxic action sites [37–40]. For example, cations were assumed to reduce toxicity in fish by competing with toxic metal ions for binding sites on gills or other biological surfaces [60]. On this basis, the biotic ligand model was developed. BLMs are metal-specific and organism-specific, requiring the incorporation of empirically determined metal-binding constants and intrinsic metal sensitivity of different biological species [44]. This shows that elevated magnesium concentrations and elevated pH result in significantly higher PNEC values, indicating lower chronic ecotoxicological effects than compliance testing by generic environmental quality standards (EQS).

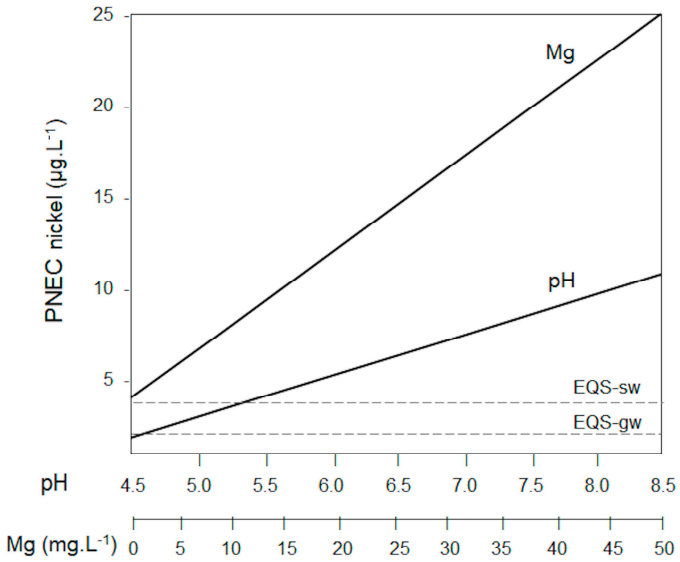


Figure 5. Predicted no-effect concentrations of nickel in pore water as a function of pH and Mg calculated via BLM. Olivine weathering increases both pH and Mg, resulting in higher (less toxic) PNEC values. Generic environmental quality standards (EQS) for nickel are 4 $\mu g \cdot L^{-1}$ for surface water (sw) and 2.1 $\mu g \cdot L^{-1}$ for groundwater (gw)(EC, 2011).

4. Conclusions

The direct relationship between reaction rate and particle size distribution was demonstrated. The concept of using the actual particle-size-specific weathering rates, instead of a monodisperse (uniform particle size) approach, showed that time-related dissolution of olivine may occur significantly faster. The total error of neglecting this effect was most pronounced in the first years due to the influence of the finest particles in a ground mineral batch. The sequestration of CO_2, following the kinetic size-dependent dissolution of olivine, may be quantified for various olivine types, doses, grain sizes, and environmental conditions. In the studied scenario, CO_2 capture by olivine dissolution was significant as a long-term means of sequestration.

The dissolution routine was coupled with sophisticated risk assessment routines (biotic ligand models) to identify the ecotoxicological effects of the release of nickel, which is incorporated in the mineral. The effect of particle size on the release of nickel was quantified. It clearly showed that larger particles reach a steady state significantly faster than fine fractions due to the slow kinetic release of Ni. This indicates that larger grain sizes may avoid the occurrence of elevated nickel concentrations in pore water, and thus reduce nickel availability to biota. Environmental impact of nickel was expressed via no-effect concentrations, showing inherent relations with pH and magnesium, which both have a detoxifying effect. The coupled models allowed for scenario analyses of olivine applications under different environmental conditions, and provided quantitative insights in weathering rates, time-related CO_2 sequestration rate, and environmental risk assessment.

Author Contributions: J.P.M.V.: conceptualization, risk assessment, model development, analysis, writing. P.K.: model development, conceptual analysis, review, and editing. All authors have read and agreed to the published version of the manuscript.

Funding: This research was funded by TKI Top Sector Energy Gas, grant number TKI2019-CCUS-CO-Action.

Institutional Review Board Statement: Not applicable.

Informed Consent Statement: Not applicable.

Data Availability Statement: Data can be made available on request, pending certain confidentiality conditions.

Acknowledgments: Jörg Gigler of the Topsector Energy-Gas (TKI) is gratefully acknowledged for his trust and support in this project. We are grateful to The Climate Knowledge Innovation Community (C-KIC) and the Rijksdienst Ondernemend Nederland (RVO) for supporting earlier stages of model development.

Conflicts of Interest: The authors declare that the research was conducted in the absence of any commercial or financial relationships that could be construed as a potential conflict of interest.

References

1. IPCC. Sixth Assessment Report. Impacts, Adaptation and Vulnerability. Intergovernmental Panel on Climate Change, WHO, UNEP. 2021. Available online: https://www.ipcc.ch/report/ar6/wg2/downloads/ (accessed on 25 September 2022).
2. Dunsmore, H.E. A geological perspective on global warming and the possibility of carbon dioxide removal as calcium carbonate mineral. *Energy Convers. Mgmt.* **1992**, *33*, 565–572. [CrossRef]
3. Bearat, H.; McKelvy, M.J.; Chizmeshya, A.V.G.; Gormley, D.; Nunez, R.; Carpenter, R.W.; Squires, L.; Wolf, G.H. Carbon sequestration via aqueous olivine mineral carbonation: Role of passivating layer formation. *Environ. Sci. Technol.* **2006**, *40*, 4802–4808. [CrossRef]
4. Schuiling, R.D.; De Boer, P.L. Coastal spreading of olivine to control atmospheric CO_2 concentrations; A critical analysis of viability. Comment: Nature and laboratory experiments are different. *Short Comm. Int. J. Greenh. Gas Control* **2010**, *4*, 855–856. [CrossRef]
5. Baumeister, J.L. Chemical Weathering of the Mafic Minerals Serpentine and Olivine in Natural Environments. UNLV Thesis, Dept. Geoscience, University of Nevada, Reno, NV, USA, 2012.
6. Hartmann, J.; West, A.J.; Renforth, P.; Koehler, P.; De La Rocha, C.L.; Wolf-Gladrow, D.A.; Duerr, H.H.; Scheffran, J. Enhanced chemical weathering as a geoengineering strategy to reduce atmospheric carbon dioxide, supply nutrients, and mitigate ocean acidification. *Rev. Geophys.* **2013**, *51*, 113–149. [CrossRef]
7. Malik, A. Kinetics of Olivine Dissolution in Column Experiments. Ph.D. Thesis, University Hamburg, Hamburg, Germany, 2017.
8. Beerling, D.J.; Leake, J.R.; Long, S.P.; Scholes, J.D.; Ton, J.; Nelson, P.N.; Bird, M.; Kantzas, E.; Taylor, L.L.; Sarkar, B.; et al. Farming with crops and rocks to address global climate, food and soil security. *Nat. Plants* **2018**, *4*, 138–147. [CrossRef] [PubMed]
9. Lehmann, J.; Possinger, A. Atmospheric CO2 removed by rock weathering. *Nature* **2020**, *583*, 204–205. [CrossRef] [PubMed]
10. Te Pas, E. Is the CO_2 Hunter a Green, Black or White Mineral? Exploring the Enhanced Weathering Potential of Olivine, Basalt, Wollastonite, Anorthite, and Albite to Improve Agricultural Production and Mitigate Climate Change. Ph.D. Thesis, Wageningen University, Wageningen, The Netherlands, 2020.
11. Schuiling, R.D.; Tickiell, O. Enhanced weathering of olivine to capture CO_2. *J. Appl. Geochem.* **2010**, *4*, 510–519.
12. Bakker, D.J.; Beumer, V.; Hartog, N.; Snijders, W.; Sule, M.; Vink, J.P.M. *Applications of Olivine in RWS Constructions; Inventory of Possibilities for Pilots*; Deltares Technical Report BGS-1203661: Utrecht, The Netherlands, 2011. (In Dutch)
13. Vink, J.P.M.; Den Hamer, D. *Olivine Captures CO_2 in the City of Rotterdam; Possibilities for Practical Applications and Climate Targets*; Deltares Technical Report 1206650: Utrecht, The Netherlands, 2012. (In Dutch)
14. World Bank. What You Need to Know About the Measurement, Reporting, and Verification (MRV) of Carbon Credits. Available online: https://www.worldbank.org/en/news/feature/2022/07/27/what-you-need-to-know-about-the-measurement-reporting-and-verification-mrv-of-carbon-credits (accessed on 11 December 2022).
15. Christoph, B.; Keel, G.; Leifeld, J. *The Role of Atmospheric Carbon Dioxide Removal in Swiss Climate Policy-Fundamentals and Recommended Actions*; Report by Risk Dialogue Foundation; Commissioned by the Federal Office for the Environment: Bern, Germany, 2019.
16. Wood, B.J.; Kleppa, O.J. Thermochemistry of forsterite-fayalite olivine solutions. *Geochim. Cosmochim. Acta* **1981**, *45*, 529–534. [CrossRef]
17. Donaldson, C.H. The rates of dissolution of olivine, plagioclase, and quartz in a basalt metl. *Mineral. Mag.* **1985**, *49*, 683–693. [CrossRef]
18. Torres, M.A.; West, A.J.; Li, G. Sulphide oxidation and carbonate dissolution as a source of CO_2 over geological timescales. *Nature* **2014**, *507*, 346–349. [CrossRef]
19. Gbor, P.K.; Jia, C.Q. Critical evaluation of coupling particle size distribution with the shrinking core model. *Chem. Eng. Sci.* **2004**, *59*, 1979–1987. [CrossRef]
20. Graff, C.P.; Wittrup, K.D. Theoretical analysis of antibody targeting of tumor spheroids: Importance of dosage for penetration and affinity for retention. *Cancer Res.* **2003**, *63*, 1288–1296. [PubMed]
21. Wanta, K.C.; Perdana, I.; Petrus, H.T.B.M. Evaluation of shrinking core model in leaching process of Pomalaa nickel laterite using citric acid as leachant at atmospheric conditions. *Mater. Sci. Eng.* **2017**, *162*, 012018. [CrossRef]
22. Wu, J.; Ahn, J.; Lee, J. Kinetic and mechanism studies using shrinking core model for copper leaching from chalcopyrite in methanesulfonic acid with hydrogen perioxide. *Miner. Process. Metall. Rev.* **2020**, *42*, 2021.

23. Safari, V.; Arzpeyma, G.; Rashchi, F.; Mostoufi, N. A shrinking particle—shrinking core model for leaching of a zinc ore containing silica. *Intl. J. Miner. Process.* **2009**, *93*, 79–83. [CrossRef]
24. Hangx, S.; Spiers, C.J. Coastal spreading of olivine to control atmospheric CO_2 concentrations: A critical analysis of viability. *Intl. J. Greenh. Gas Control* **2009**, *3*, 757–767. [CrossRef]
25. Pokrovsky, O.S.; Schott, J. Kinetics and mechanism of forsterite dissolution at 25C and pH from 1 to 12. *Geochim. Cosmochim. Acta* **2000**, *64*, 3313–3325. [CrossRef]
26. White, A.F.; Blum, A.E.; Bullen, T.D.; Vivit, D.V.; Schulz, M.; Fitzpatrick, J. The effect of temperature on experimental and natural chemical weathering rates of granitoid rocks. *Geochim. Cosmochim. Acta* **1999**, *63*, 3277–3291. [CrossRef]
27. Nagy, K.L.; Blum, A.E.; Lasaga, A.C. Dissolution and precipitation kinetics of kaolinite at 80 degrees C and pH 3; the dependence on solution saturation state. *Am. J. Sci.* **1991**, *291*, 649–686. [CrossRef]
28. Holdren, G.R.; Speyer, P.M. Reaction rate-surface area relationships during the early stages of weathering 1. *Geochim. Cosmochim. Acta* **1985**, *49*, 675–681. [CrossRef]
29. Palandri, J.L.; Kharaka, Y.K. *A compilation of Rate Parameters of Water-Mineral Interaction Kinetics for Application to Geochemical Modelling*; Technical Report by the US Geological Survey: Reston, VA, USA, 2004.
30. Olsen, A.A. Forsterite Dissolution Kinetics: Applications and Implications for Chemical Weathering. Ph.D. Thesis, Faculty Virginia Polytechnic Institute State University, Blacksburg, VA, USA, 2007.
31. Vink, J.P.M.; Giesen, D.; Ahlrichs, E. Olivine weathering in field trials. In *Effect of Natural Environmental Conditions on Mineral Dissolution and the Potential Toxicity of Nickel*; Deltares Technical Report 11204378: Utrecht, The Netherlands, 2022.
32. Vink, J.P.M.; Meeussen, J.C.L. BIOCHEM-ORCHESTRA: A scenario-DSS for heavy metal speciation and ecotoxicological impacts in river systems. *Environ. Poll.* **2007**, *148*, 833–841. [CrossRef] [PubMed]
33. SCHER. *Opinion on the Chemicals and the Water Framework Directive: Technical Guidance for Deriving Environmental Quality Standards*; Scientific Committee on Health and Environmental Risks, European Union: Brussels, Belgium, 2010.
34. Schlekat, C.E.; Van Genderen, E.; DeSchamphelaere, K.A.C.; Antunes, P.M.C.; Rogevich, E.C.; Stubblefield, W.A. Cross-species extrapolation of chronic nickel biotic ligand models. *Sci. Total Environ.* **2010**, *408*, 6148–6157. [CrossRef] [PubMed]
35. Verschoor, A.; Vink, J.P.M.; Vijver, M.G.; De Snoo, G. Geographical and temporal variation in Cu, Zn, Ni bioavailability and species sensitivity. *Environ. Sci. Technol.* **2011**, *45*, 6049–6056. [CrossRef]
36. Rüdel, H.; Díaz Muñiz, C.; Garelick, H.; Kandile, N.; Miller, B.; Pantoja Munoz, L.; Peijnenburg, W.G.M.; Purchase, D.; Shevah, Y.; Van Sprang, P.; et al. Consideration of the bioavailability of metal/metalloid species in freshwaters: Experiences regarding the implementation of biotic ligand model-based approaches in risk assessment frameworks. *Environ. Sci. Pollut. Res.* **2015**, *22*, 7405–7421. [CrossRef]
37. Pagenkopf, G.K. Gill surface interaction model for trace-metal toxicity to fishes: Role of complexation, pH and water hardness. *Environ. Sci. Technol.* **1983**, *17*, 342. [CrossRef]
38. Playle, R.C.; Dixon, D.G. Copper and Cadmium binding to fish gills: Estimates of Metal-Gill Stability constants and modelling of metal accumulation. *Can. J. Fish. Aquat. Sci.* **1993**, *50*, 2678. [CrossRef]
39. Di Toro, D.M.; Allen, H.E.; Bergman, H.L.; Meyer, J.S.; Paquin, P.R.; Santore, R.C. Biotic ligand model of the acute toxicity of metals. 1. Technical basis. *Environ. Toxicol. Chem.* **2001**, *20*, 2383. [CrossRef]
40. De Schamphelaere, K.A.C.; Lofts, S.; Janssen, C.R. Bioavailability models for predicting acute and chronic toxicity of zinc to algae, daphnids, and fish in natural surface water. *Environ. Toxicol. Chem.* **2005**, *24*, 1190. [CrossRef]
41. European Commission. *Common Implementation Strategy for the Water Framework Directive (2000/60/EC) Guidance Document No. 27 Technical Guidance for Deriving Environmental Quality Standards*; European Communities: Brussels, Belgium, 2011.
42. European Commission. *Science for Environment Policy. Advances in Fresh Water Risk Assessment: Experiences with Biotic Ligand Models*; European Communities: Brussels, Belgium, 2016; Issue 441.
43. European Union. *Guidance Document No. 38 Technical Guidance for Implementing Environmental Quality Standards (EQS) for Metals*; Consideration of metal bioavailability and natural background concentrations in assessing compliance. 2000/60/EC; European Union: Brussels, Belgium, 2019.
44. European Union. *European Union Risk Assessment Report. Nickel and Nickel Compounds*; Prepared by The Danish Environmental Protection Agency, on behalf of the European Union. Health and Consumer Protection DC, B-1049; European Union: Brussels, Belgium, 2008.
45. Verschoor, A.; Vijver, M.G.; Vink, J.P.M. Refinement and cross-validation of nickel bioavailability in PNEC-pro, a regulatory tool for site-specific risk assessment of metals in surface waters. *Environ. Toxicol. Chem.* **2017**, *36*, 2367–2376. [CrossRef]
46. Vink, J.P.M.; Verschoor, A.; Vijver, M.G. PNEC-pro. Software Release Version 6. Available online: http://www.pnec-pro.com (accessed on 25 September 2016).
47. Kremer, D.; Etzold, J.S.; Boldt, P.; Blaum, K.M.; Hahn, H.; Wotruba, R. Telle Geological mapping and characterization of possible primary input materials for the mineral sequestration of carbon dioxide in Europe. *Minerals* **2019**, *9*, 485. [CrossRef]
48. NIST/SEMATECH e-Handbook of Statistical Methods. 2021. Available online: https://www.itl.nist.gov/div898/handbook/ (accessed on 23 April 2021). [CrossRef]
49. Renforth, P.; Von Strandmann, P.A.E.; Henderson, G.M. The dissolution of olivine added to soil: Implications for enhanced weathering. *Appl. Geochem.* **2015**, *61*, 109–118. [CrossRef]

50. Köhler, P.; Abrams, J.F.; Völker, C.; Hauck, J.; Wolf-Gladrow, D.A. Geoengineering impact of open ocean dissolution of olivine on atmospheric CO2 surface ocean pH and marine biology. *Environ. Res. Lett.* **2013**, *8*, 014009. [CrossRef]
51. Montserrat, F.; Renforth, P.; Hartmann, J.; Leermakers, M.; Knops, P.; Meysman, P.J.R. Olivine dissolution in seawater; implications for CO2 sequestration through enhanced weathering in coastal environments. *Environ. Sci. Technol.* **2017**, *51*, 3960–3972. [CrossRef]
52. Amann, T.; Hartmann, J.; Struyf, E.; De Oliveira Garcia, W.; Fisher, E.K.; Janssens, I.; Meire, P.; Schoelynck, J. Constraints on enhanced weathering and related carbon sequestration: A cropland mesocosm approach. *Biogeosciences* **2020**, *17*, 103–119. [CrossRef]
53. Dietzen, C.; Harrisona, R.; Michelsen-Correac, S. Effectiveness of enhanced mineral weathering as a carbon sequestration tool and alternative to agricultural lime: An incubation experiment. *Int. J. Greenh. Gas Control* **2018**, *74*, 251–258. [CrossRef]
54. Bach, L.T.; Gill, S.J.; Rickaby, R.E.M.; Gore, S.; Renforth, P. CO_2 removal with enhanced weathering and ocean alkalinity enhancement: Potential risks and co-benefits for marine pelagic ecosystems. *Front. Clim.* **2019**, *1*, 1–21. [CrossRef]
55. Kersbergen, G. *The possibilities of Olivine Enhanced Weathering in Paved Road Construction. A Literature Review*; Technical report nr. 4233670; Utrecht University: Utrecht, The Netherlands, 2020.
56. Haque, F.; Chiang, Y.W.; Santos, R.M. Risk assessment of Ni, Cr, and Si release from alkaline minerals during enhanced weathering. *Open Agric.* **2020**, *5*, 166–175. [CrossRef]
57. Campbell, D.J. Interactions between trace metals and aquatic organisms: A critique of the free ion activity model. In *Metal Speciation and Bioavailability in Aquatic Systems*; Tessier, A., Turner, D., Eds.; John Wiley: New York, NY, USA, 1995; pp. 45–102.
58. Vink, J.P.M. Measurement of heavy metal speciation over redox gradients in natural water-sediment interfaces and implications for uptake by benthic organisms. *Environ. Sci. Technol.* **2002**, *36*, 5130–5138. [CrossRef] [PubMed]
59. Vink, J.P.M. The origin of speciation: Trace metal kinetics and bioaccumulation by Oligochaetes and Chironomids in undisturbed water-sediment interfaces. *Environ. Pollut.* **2009**, *157*, 519–527. [CrossRef]
60. Erickson, R.J. The biotic ligand model approach for addressing effects of exposure water chemistry on aquatic toxicity of metals: Genesis and challenges. *Environ. Toxicol. Chem.* **2013**, *32*, 1212. [CrossRef]

Disclaimer/Publisher's Note: The statements, opinions and data contained in all publications are solely those of the individual author(s) and contributor(s) and not of MDPI and/or the editor(s). MDPI and/or the editor(s) disclaim responsibility for any injury to people or property resulting from any ideas, methods, instructions or products referred to in the content.